Received May 22, 2020, accepted June 11, 2020, date of publication June 18, 2020, date of current version June 30, 2020.

Digital Object Identifier 10.1109/ACCESS.2020.3003521

A Novel PSOS-CGSA Method for State Estimation in Unbalanced DG-Integrated Distribution Systems

ZIA ULLAH[1], (Graduate Student Member, IEEE), MOHAMED R. ELKADEEM[1,2], (Graduate Student Member, IEEE), SHAORONG WANG[1], AND JORDAN RADOSAVLJEVIĆ[3]

[1]State Key Laboratory of Advanced Electromagnetic Engineering and Technology, Huazhong University of Science and Technology, Wuhan 430074, China
[2]Department of Electrical Power and Machines Engineering, Faculty of Engineering, Tanta University, Tanta 31521, Egypt
[3]Faculty of Technical Sciences, University of Priština at Kosovska Mitrovica, 38220 Kosovska Mitrovica, Serbia

Corresponding author: Zia Ullah (ziaullah@hust.edu.cn)

This work was supported by the National Key research and Development Program of China under Grant 2017YFB0902800.

ABSTRACT This paper proposes a novel optimization method, namely, hybrid PSOS-CGSA for state estimation in three-phase unbalanced DG-integrated distribution systems. The distribution system state estimation (DSSE) is formulated as a nonlinear optimization problem with constraints where loads and DG outputs are considered as the control variables, while real-time measurements are treated as dependent variables. The proposed DSSE model estimates the loads and DG outputs at each bus by minimizing the difference between the measure and calculated values of the variables monitored in real-time. A novel hybrid algorithm of particle swarm optimization with sigmoid-based acceleration coefficients and chaotic gravitational search algorithm (PSOS-CGSA) is proposed and applied for the DG-integrated DSSE. The feasibility of the proposed approach is verified on the IEEE 13-bus test system, the IEEE 37-bus test system, and the IEEE 123-bus test system. These simulations show that the proposed DSSE model provides reliable and accurate state estimation of DG-integrated distribution systems with a very limited number of real-time measurements at the source substation. The results obtained by proposed hybrid PSOS-CGSA are evaluated by comparing with other methods under the same test conditions, and the obtained results demonstrate the merits of the proposed scheme.

INDEX TERMS Hybrid intelligent algorithm, metaheuristic optimization, state estimation, unbalanced distribution system.

I. INTRODUCTION

A. MOTIVATION AND INCITEMENT

The advent and growing integration of distributed generators into the electric power distribution networks transform conventional distribution networks into smart DG-integrated systems. The penetration of DGs has various implications on the power system behaviour such as change in the power flow and voltage deviation at buses. However, it has been widely used in the distribution networks. Such new challenges and the trend heading towards DG-integrated power systems both need more detailed and accurate knowledge of the distribution power networks states to incorporate real-time monitoring and state estimation for DG-integrated systems.

The state estimation in the power system is a mathematical algorithm that, at a given moment, based on available measurements, provides reliable and the best estimation of voltages and other variables relevant to system operation. State estimation is an essential function in the process of analysis, control, and management of power systems. On the other hand, the system state estimation in transmission lines is based on a redundant set of telemetry measurements. For transmission systems, there is always the assumption of symmetrical and balanced operation, so that all calculations are performed on the corresponding single-phase positive sequence models [1]. However, distribution networks have many specifics in comparison to transmission networks,

The associate editor coordinating the review of this manuscript and approving it for publication was Taha Selim Ustun.

such as radial topology, un-transposed three-phase feeders (with two-phase and single-phase laterals having high r/x ratios), unbalanced loads, and a small number of real-time measurements. Under these specifics, the state estimation techniques for transmission networks cannot be applied directly to distribution networks, which means that three-phase state estimation is necessary. A unique feature of distribution system state estimation (DSSE) is the small number of real-time measurements. In such a situation, it is necessary for introducing pseudo measurements, which refer to active and reactive powers of loads and distributed generation (DG) to achieve the system observability. The general framework for defining and solving the DSSE problem must include the following aspects:

- Three-phase models of distribution system components, including lines, transformers, loads, and DG.
- Availability of real-time measurement.
- Inclusion and modeling of pseudo-measurements. Defining state variables and DSSE problem formulation. DSSE algorithm for determining the state variables.

So far, many authors have dealt with the DSSE problem focusing on all or some of the above issues. The authors [2]–[4] give comprehensive reviews of different issues related to DSSE. In accordance with these considerations, there are three DSSE paradigms: WLS-based DSSE, load adjustment DSSE methods, and robust DSSE methods.

B. LITERATURE REVIEW

Recently, several innovative research approaches have been proposed for the DSSE. In paper [5], Ranković *et al.* proposed an improved WLS based three-phase SE algorithm for unbalanced distribution systems, where the vector of state variables comprises the components of complex voltages combined with variables associated with the classification of integrated DG units. In [6], a detailed representation of the ground loops in the model of an active unbalanced distribution network suitable to three-phase state estimation is introduced. Starting from the characteristics of distribution networks related to small voltage differences between two busses of each line segment, the authors [7], [8] casted the state estimation problem into a sparse vector recovery problem. A branch-current-based WLS with a new technique aims to process the data obtained from smart metering is proposed in [9], where the main objective of the proposed scheme is to execute the three-phase DSSE accurately. Othman *et al.* proposed a DSSE model considering DG integration in distribution networks [10]. This technique is based on updating the complex power flow in the overall network according to the online measurement from smart meters positioned at specific locations dependent on the network topology only. A three-phase DSSE methodology for unbalanced radial distribution networks is presented in [11], the proposed method uses the load regulation via active utilization and imbalance factors. In [12], the authors also proposed a three-phase DSSE algorithm based on load correction. This approach uses real-time measurements at the substation and pseudo-measurements generated from the customers' energy bills. Several authors proposed artificial neural networks (ANN)-based DSSE algorithms to overcome a limited number of measurements in distribution networks [13], [14]. Cheng *et al.* [15] combined extreme machine learning with a genetic algorithm to predict the photovoltaic generation and used it as a pseudo-measurement in a WLS-based DSSE algorithm. Considering the problem of SE as a global optimization problem with constraints, some authors have suggested metaheuristic-based methods for solving it. A cooperative particle swarm optimization (Co-PSO) algorithm is proposed in [16] for DSSE in unbalanced three-phase distribution networks with renewable DGs. Nanchian *et al.* [1] have demonstrated the application of a hybrid particle swarm optimization (HPSO) for three-phase DSSE, including the on-load tap changer positions for voltage control. In [17], the authors proposed a hybrid DSSE technique using the WLS method and firefly algorithm (FA) for distribution networks with integrated renewable energy sources.

C. CONTRIBUTION AND PAPER ORGANIZATION

This paper proposes a new three-phase DSSE paradigm based on metaheuristic optimization. In comparison with recent literature, the main contributions of this research are as follows:

- Defining a generic research framework for three-phase DG-integrated DSSE using a novel PSOS-CGSA method.
- Application and implementation of a new hybrid PSOS-CGSA algorithm to solve the DSSE problem.
- Defining pseudo-measurements for renewable-based DG units using forecasted output powers.

The rest of this paper is organized as follows: Section II presents the three-phase power flow and modeling of power system components. The problem formulation has described in Section III. Section IV presents the application of the proposed PSOS-CGSA method for DG-integrated DSSE. Investigated test cases and method validation along with detail simulation results and discussion are presented in Section V. Finally; Section VI concludes the studied research of this paper.

II. THREE-PHASE POWER FLOW

The power flow calculation is an essential function of each DSSE algorithm, regardless of its paradigm. This paper uses the well-known backward/forward power flow algorithm. The backward/forward method is based on two sweeps of calculations. In the backward sweep, the bus voltages are identified for the first iteration, and currents are calculated starting from the branches connected to the far buses and solved up to the source bus by applying the Kirchhoff's first law. In the forward sweep, starting from the branches connected to the source bus and moving toward the ending branches, the voltages at the receiving buses are calculated using the voltages at corresponding sending buses and the branch currents calculated from the backward sweep. The voltages from the forward sweep are used for the next iteration in the backward sweep calculations [18]. Convergence occurs when the voltage mismatch for all phases at each bus becomes smaller than a convergence criterion. However, it should be noted that proper three-phase modeling of the distribution network components is crucial for the efficiency and accuracy of the power flow calculations.

A. LINE MODELLING

Since the distribution network consists of un-transposed three-phase, two-phase and single-phase lines with a mainly unbalanced load, it is necessary to take into account the magnetic coupling between the phases of the lines as well as the influence of the earth as a return path of the unbalance current. In addition, due to the uneven geometric position of the phases, the mutual phase capacities and the influence of the earth on the capacitance of the lines should be taken into account. Therefore, the lines in distribution networks should be modeled by the (3 × 3)-dimensional three-phase series impedance and shunt admittance matrices. The calculation of these two matrices is based on the Carson equations and Kr on reductions, as detail explained in [19].

B. TRANSFORMER MODELLING

The first problem in applying the backward/forward sweep-based power flow method for the unbalanced radial distribution networks with multiple voltage levels is reflected in the inability of direct summarizing branch currents (backward sweep) and calculating the bus voltages (forward sweep) for three-phase transformer whose secondary windings connections are delta or ungrounded wye. In this paper, the symmetrical components model with appropriate transfer matrices for different connection types of transformers is used to overcome this problem.

C. LOAD MODELLING

The loads in distribution networks can be three-phase, two-phase, or single-phase, connected in grounded wye (Y) or ungrounded delta (Δ) configuration, and considered to be line-to-neutral for Y and line-to-line for Δ connection [19]. In the power flow calculation, the line currents are relevant, which is the currents per network phases. In addition to the load configuration (Y or Δ), the calculation of these currents also depends on the load model. The loads in distribution networks are usually modeled from the point of view of the dependence of power with voltage. There are used three models: constant power (PQ), constant impedance (Z) and constant current (I), or any combination of the three.

D. DISTRIBUTED GENERATION MODELLING

The bus with DG can be represented as a PQ or PV bus. In case the bus i is modeled as a PQ bus, the DG unit should be treated as negative PQ load. In case the DG units modeled as PV buses, the power flow algorithm requires some additional processes related to calculating the reactive power injections at the PV buses needed to achieve the specified voltage magnitudes [18].

III. FORMULATION OF DSSE

The following types of measurements are available in most distribution networks [5], [20].

- Real-time measurements at the source, i.e., at the secondary side of distribution substation: source bus voltage magnitude, active and reactive powers, current magnitudes and power factors
- Real-time measurements at selected points of the distribution network using remote control units: voltages, powers, currents.
- Real-time measurements at monitored (dispatch-able) DG units: bus voltage and active power injection
- Pseudo-measurements of loads based on historical data and typical daily load diagrams
- Pseudo-measurements at unmonitored DG units based on the external inputs such as historical database and/or weather forecast

DSSE algorithm should enable the determination of the entire network state for specified the network topology, the real-time measurements as well as known historical data about loads and unmonitored DG units. On the other hand, the problem of DSSE can be represented as a nonlinear optimization problem with constraints, where the loads and DG outputs can be considered as the control variables, and the real-time measurement variables are dependent variables. This means that the DSSE algorithm estimates the loads and DG outputs at each bus by minimizing the difference between the measured and calculated values of the variables monitored in real-time. Therefore, the objective function of the DSSE can be expressed as follows:

$$\min f(\mathbf{x}, \mathbf{y}) = \sum_{i=1}^{m} |z_i - h_i(\mathbf{x}, \mathbf{y})| \tag{1}$$

where $\mathbf{x}$ is the vector of control variables, $\mathbf{y}$ is the vector of dependent variables, z_i is the measured value of the real-time measurement variable i, h_i is the nonlinear measurement function for the real-time measurement variable i, and m is the total number of real-time measurements.

The control variables are active and reactive power of loads and active and reactive power outputs of unmonitored DG units. Assuming that the power factor of loads and power factor of unmonitored DG units be constant, the vector $\mathbf{x}$ can be expressed as:

$$\mathbf{x} = [\mathbf{P}_{abc,L1}, \mathbf{P}_{abc,L2}, \ldots, \mathbf{P}_{abc,LN_L}, \mathbf{P}_{abc,DG1}, \mathbf{P}_{abc,DG2}, \ldots, \mathbf{P}_{abc,DGN_{UMDG}}] \tag{2}$$

where $\mathbf{P}_{abc,Li} = \begin{bmatrix} P_{a,Li} & P_{b,Li} & P_{c,Li} \end{bmatrix}^T$ is the vector of three-phase power of load at the ith bus, $\mathbf{P}_{abc,DGi} = \begin{bmatrix} P_{a,DGi} & P_{b,DGi} & P_{c,DGi} \end{bmatrix}^T$ is the vector of the three-phase power output of DG at the ith bus, N_L is the number of load buses, and N_{UMDG} is the number of unmonitored DG units.

The vector of dependent variables consists of active power delivered through the root bus of the distribution network, voltage magnitude off all the buses of the network, and branch power flow:

$$\mathbf{y} = [\mathbf{V}_{abc,1}, \mathbf{V}_{abc,2}, \ldots, \mathbf{V}_{abc,N}, \mathbf{S}_{abc,1}, \mathbf{S}_{abc2}, \ldots, S_{abc,N}] \tag{3}$$

where $\mathbf{V}_{abc,i} = \left[\, V_{a,i} \; V_{b,i} \; V_{c,i} \,\right]^T$ is the vector of three-phase voltage magnitude at the ith bus, $\mathbf{S}_{abc,i} = \left[\, S_{a,i} \; S_{b,i} \; S_{c,i} \,\right]^T$ is the vector of three-phase power flow through the ith branch, N is the number of buses.

The equality constraints are the nonlinear power flow equations described in Section II.

The functional operating constraints are the lower and upper limits of each dependent variable, as follows:

$$\mathbf{V}^{\min}_{abc,i} \leq \mathbf{V}_{abc,i} \leq \mathbf{V}^{abc}_{abc,i} \tag{4}$$

$$\mathbf{S}^{\min}_{abc,i} \leq \mathbf{S}_{abc,i} \leq \mathbf{S}^{abc}_{abc,i} \tag{5}$$

The inequality constraints of control variables define the feasibility region of the DSSE problem:

$$\mathbf{P}^{\min}_{abc,Li} \leq \mathbf{P}_{abc,Li} \leq \mathbf{P}^{\max}_{abc,Li} \tag{6}$$

$$\mathbf{P}^{\min}_{abc,DGi} \leq \mathbf{P}_{abc,DGi} \leq \mathbf{P}^{\max}_{abc,DGi} \tag{7}$$

A. LIMITS OF LOADS AS CONTROL VARIABLES

In DSSE, the loads are considered as pseudo-measurements. The pseudo-measurement values represent the forecasted mean values with added measurement noise, as follows:

$$\mathbf{P}^{pm}_{abc,Li} = \mathbf{P}^{0}_{abc,Li} + (2r-1)\,\mathbf{P}^{0}_{abc,Li}\frac{e_{pm}}{100} \tag{8}$$

Now, the upper and lower load limits in (6) can be calculated as:

$$\mathbf{P}^{\max,\min}_{abc,Li} = \mathbf{P}^{pm}_{abc,Li}\left(1 \pm \frac{e_{pm}}{100}\right) \tag{9}$$

where $\mathbf{P}^{0}_{abc,Li}$ is the forecasted value of load power at bus i, r is a random number uniformly distributed in the range [0,1], e_{pm} is the error in (%) adopted for the pseudo-measurements.

Calculation of the forecasted value of load ($\mathbf{P}^{0}_{abc,Li}$) is based on historical data [21]:

- Daily load profile for active power normalized by average or peak values.
- The load weight, which can be: peak value based on field measurement, the average value derived from supplied energy, or only rated power of the equipment.

The forecasted value of load ($\mathbf{P}^{0}_{abc,Li}$) at any moment can be obtained by multiplying the value from the daily load profile (for the selected moment) with corresponding load weight. Typical daily load profiles ere established for different consumption types, such as industrial, commercial, and residential. In addition, each consumption type is presented with a characteristic daily load profile and corresponding load weight for typical loading days (week-day, weekend, holiday) in each weather season (spring, summer, fall, winter).

B. LIMITS OF DG OUTPUTS

Active power outputs of unmonitored DG units are treated as control variables, which lower and upper limits in (7) can be calculated as follows:

$$\mathbf{P}^{\max,\min}_{abc,DGi} = \mathbf{P}^{pm}_{abc,DGi}\left(1 \pm \frac{e_{pm}}{100}\right) \tag{10}$$

where $\mathbf{P}^{pm}_{abc,Li}$ is the pseudo-measurement value of the DG output power at the bus i, which is calculated as follows:

$$\mathbf{P}^{pm}_{abc,DGi} = \mathbf{P}^{0}_{abc,DGi} + (2r-1)\,\mathbf{P}^{0}_{abc,DGi}\frac{e_{pm}}{100} \tag{11}$$

where $\mathbf{P}^{0}_{abc,DGi}$ is the forecasted output power of the ith DG unit, at a given moment of interest. Detail procedures for calculating the forecasted output powers of renewable-based DG units, such as wind turbine (WTG) and photovoltaic (PVG), can be found in [22].

C. REAL-TIME MEASUREMENTS

As noted above, the real-time measurements (z_i) are performed for voltage magnitudes and power flows at the substation, and voltage magnitudes and power flows at selected points of the distribution network. The maximum error of 3% is considered for these real-time measurements. Therefore, the real-time measurement respecting the measurement error can be simulated by introducing random noise in the true value, as follows:

$$\mathbf{M}^{rt}_{abc,i} = \mathbf{M}^{0}_{abc,i} + (2r-1)\,\mathbf{M}^{0}_{abc,i}\frac{e_{rt}}{100} \tag{12}$$

where $\mathbf{M}^{0}_{abc,i}$ is the true value of a variable (voltage, power, etc.), and e_{rt} is the error in (%) adopted for the real-time measurements, and $\mathbf{M}^{rt}_{abc,i}$ is the measured value of a three-phase variable, respecting the measurement error.

IV. PROPOSED PSOS-CGSA METHOD FOR DG-INTEGRATED DSSE

In this paper, an innovation of the well-known hybrid PSOGSA algorithm [23], namely a hybrid PSOS-CGSA algorithm, is proposed to effectively solve the DSSE problem. Our proposed hybrid PSOS-CGSA algorithm based on the hybridization of particle swarm optimization with sigmoid-based acceleration coefficients (PSOS) [24] and chaotic gravitational search algorithm (CGSA) [25]. The improvements of PSOS-CGSA in relation to the original PSOGSA algorithm is based on modeling the cognitive and social acceleration coefficient (C_1 and C_2) with a new sigmoid-based acceleration coefficient, and introduction of a chaos sinusoidal map into the gravitational constant (G). These actions improve both exploration and exploitation phases of the proposed hybrid algorithm by balancing the global search ability in the early stage and the global convergence in the later stage.

Since the proposed hybrid PSOS-CGSA algorithm belongs to metaheuristic population-based optimization techniques, it will be explained here through a general metaheuristic framework [26].

The metaheuristic optimization methods are built upon population-based stochastic search algorithms. By population (POP), we mean a set of search agents of size (N), representing the possible solutions of the problem. The search agents are denoted by a vector (xi) of length (n) where the entries of the vector are the values of the relevant control variables. The length of the vector is also a measure of the search space dimension of the given optimization problem. In other words, the metaheuristic methods iteratively approximate the solution to the problem. At each stage, a new population is generated after applying the search operators on agents in the current population. The main structure of our proposed algorithm is based on the following procedure described as follows:

Defining and Initialization Procedure:

1. Define objective function $F(\mathbf{x_i})$ and possible solutions space **X;**
2. Generate N agents, and assign the starting position randomly to agents using the control variable values in the range of maximum to minimum, where the iteration counter: $t = 1$

Iterative Procedure:

1. Estimate the fitness rate for each agent in the current population $\mathbf{POP}(t)$.
2. Generate new $\mathbf{POP}(t+1)$using algorithmic operators on search agents from the $\mathbf{POP}(t)$. For the proposed hybrid PSOS-CGSA algorithm, the operators for updating the current velocity and the current position of agents are as follows:

$$\begin{aligned}\mathbf{v}_i(t+1) &= r_1 \cdot \mathbf{v}_i(t) + r_2 \cdot C_1(t) \cdot \mathbf{a}_i(t) \\ &\quad + r_3 \cdot C_2(t) \cdot (\mathbf{gbest}(t) - \mathbf{x}_i(t)) \qquad (13)\\ \mathbf{x}_i(t+1) &= \mathbf{x}_i(t) + \mathbf{v}_i(t+1) \qquad (14)\end{aligned}$$

The cognitive and social acceleration coefficients are updated in each iteration using the following equations [24]:

$$C_1(t) = \frac{1}{1+\exp\left(-\lambda \cdot \frac{t}{t_{\max}}\right)} + 2\left(C_{1f} - C_{1i}\right)\left(\frac{t}{t_{\max}} - 1\right)^2 \qquad (15)$$

$$C_2(t) = \frac{1}{1+\exp\left(-\lambda \cdot \frac{t}{t_{\max}}\right)} + 2\left(C_{1f} - C_{1i}\right)\left(\frac{t}{t_{\max}}\right)^2 \qquad (16)$$

In (13), **gbest** denotes the best solution (position) among all agent's best positions achieved so far. The acceleration of agents ($\mathbf{a}_i$) is updated in each iteration, considering the gravitational constant (G) with the embedded sinusoidal chaotic map, as explained in [25]. r_1, r_2, and r_3 are random numbers in the range of [0,1], $t_{\max}$ is the maximum number of iterations, λ is a control parameter ($\lambda = 0.0001$), C_{1i} and C_{1f} are two positive constants ($C_{1i} = 0.5$, $C_{1f} = 2.5$).

5. Repeat the iterative procedure until the stop criteria is reached.
6. Report the best solution. End.

The general flowchart of our proposed algorithm is presented in Figure 1, which shows the entire process involved in the execution of PSOP-GSA algorithm for the best optimal solution.

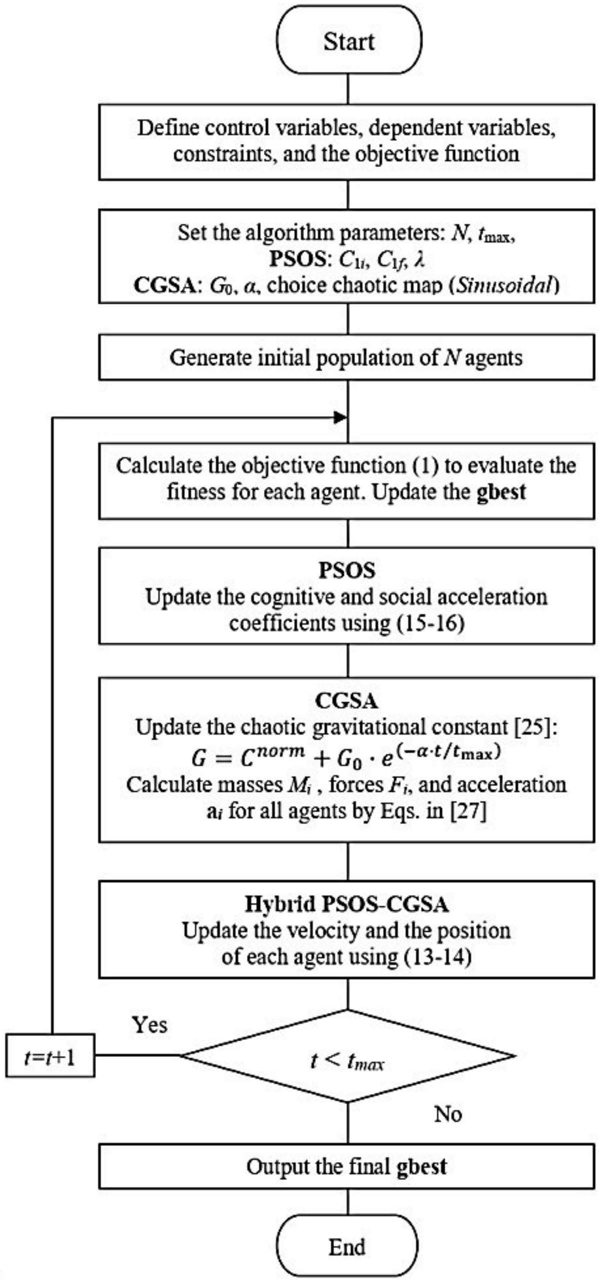

FIGURE 1. Flowchart of the proposed algorithm.

The above flow chart describes the entire execution of the proposed algorithm for the optimal results, where the proposed hybrid PSOS-CGSA approach has been applied to solve the DSSE problem in the DG-integrated distribution systems. The detailed step by step execution of PSOS-CGSA for the adaption of the optimal solution is explained in the next section:

A. APPLICATION OF PSOS-CGSA FOR DG-INTEGRATED DSSE

In the DSSE, the objective function is the minimization of absolute differences between the measured values and the estimated values, which are functions of control and dependent state variables (1). The control variables are active and reactive power of loads and active and reactive power outputs of unmonitored DG units. Therefore, a search agent, i.e., a potential solution of the DSSE can be represented based on the vector (14), as follows:

$$\mathbf{x}_i = [\mathbf{P}^1_{abc,L1}, \ldots, \mathbf{P}^d_{abc,LN_L}, \mathbf{P}^{d+1}_{abc,DG1}, \ldots, \mathbf{P}^n_{abc,DGN_{UMDG}}] \quad i = 1, \ldots, N \qquad (17)$$

where n is the number of control variables ($n = N_L + N_{UMDG}$), N is the number of agents (size of the population).

The presentation of the proposed hybrid PSOS-CGSA algorithm in solving three-phase DG-integrated DSSE can be summarized as below steps:

Step 1: Detect the input parameters, including the distribution network configuration, lines data, transformers data, and historical data related to loads and distributed generation.

Step 2: Define (read) the values of real-time measurements (z_i). Define the error of real-time measurements. Simulate the error in the real-time measurements (12).

Step 3: Define the typical daily load profiles and load weights for each of season. Calculate the forecasted values of load powers at the given moment of interest.

Step 4: Calculate the forecasted output powers of unmonitored DG units at the given moment of interest.

Step 5: Define the error of pseudo-measurements. Calculate the pseudo-measurements using (8) and (11).

Step 6: Specify the objective function (1); specify the control variables (2) and calculate their limits (9)-(10); specify the dependent variables (3) and their limits;

Step 7: Set the PSOS-CGSA algorithmic parameters; generate an initial random population of N agents; set iteration counter $t = 1$.

Step 8: Perform power flow calculation and evaluate the objective function for each agent $\mathbf{x}_i(t)$ from the current population $\mathbf{POP}(t)$;

Step 9: Apply the PSOS-CGSA operators (13)-(16) to create a new population of agents (i.e., updated solutions of the problem).

Step 10: Repeat steps 8-9 until the stop criteria is reached, i.e., the max number of iterations.

Step 11: Report the optimal results: best agent $\mathbf{x}_i$ in the last iteration - the estimated values of control variables (power of loads and power of DG units). Based on these estimated values of loads and DG outputs, a final load flow calculation is performed to estimate the values of the dependent variables: bus voltages, branch power flows, and power losses.

V. TEST CASES VALIDATION

The proposed three-phase DSSE methodology for unbalanced distribution networks is implemented in the MATLAB programming environment and validated on three representative IEEE test systems. The first one is the IEEE 13-bus system, the second one is the IEEE 37-bus system, and the third one is the IEEE 123-bus system [28]. These three test systems are simplified to key features of the DSSE algorithm be highlighted:

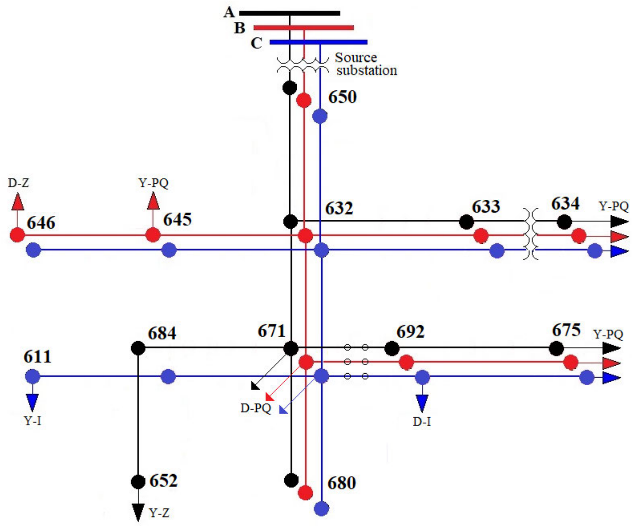

FIGURE 2. Three-phase diagram of the IEEE 13-bus test system.

- The voltage regulators are omitted, and switches in the line segments are closed
- The distributed load along the line segment is lumped and placed on half of the line.
- Shunt capacitor banks are omitted.

The three-phase power flow program was developed based on the algorithm and component models described in Section II. This program is used for the power flow computation in the test systems.

The results of the power flow computation are considered as the true system states. Real-time measurements are simulated by adding the normally distributed noise as given in (12). It is assumed that the pseudo-measurement error (e_{pm}) is 20%, while the real-time measurement error (e_{rt}) is 3%. The accuracy of the estimated states, as well as the performance of the DSSE algorithms, is evaluated using the mean absolute percentage error (MAPE), as given below:

$$MAPE(\%) = \frac{100}{n} \sum_{i=1}^{n} \left| \frac{x_i^{true} - x_i^{est}}{x_i^{true}} \right| \qquad (18)$$

where x_i^{true} and x_i^{est} are the true and estimated value of the ith variable, n is the number of considered variables.

A. IEEE 13-BUS TEST SYSTEM

The IEEE 13-bus test system is a small-size radial and highly unbalanced distribution feeder operating at 4.16 kV. The three-phase configuration of the system under study is presented in Figure 2.

The active and reactive powers of load given in [28] are considered as the forecasted mean values, which are used to generate pseudo-measurements according to (8). The power flow results represent "the true system state." It is supposed that there are available the real-time measurements of active/reactive power flows and bus voltages.

TABLE 1. IEEE 13-bus system power flow.

Bus i	Bus j	Phase A P (kW)	Phase A Q (kVAr)	Phase B P (kW)	Phase B Q (kVAr)	Phase C P (kW)	Phase C Q (kVAr)
650	632	1211.2	790.0	969.3	571.8	1267.4	862.5
632	633	162.9	115.3	121.6	92.9	121.8	93.3
633	634	159.9	109.9	120.0	89.9	119.9	89.9
632	645	-	-	311.8	127.0	66.5	117.6
645	646	-	-	141.6	1.9	66.3	117.4
632	671	1022.1	580.9	471.9	307.8	915.9	513.2
671	680	-	-	-	-	-	-
671	692	529.8	305.6	67.8	59.9	403.8	235.7
692	675	484.9	189.9	68.0	59.9	289.9	211.9
671	684	105.4	70.5			147.6	69. 7
684	611	-	-	-	-	147.1	69.2
684	652	104.7	70.3	-	-	-	-

TABLE 2. Simulation results of DSSE for the IEEE 13-bus system: MAPEV(%).

Case	Real-time measurements	Proposed PSOS-CGSA min	Proposed PSOS-CGSA max	Proposed PSOS-CGSA mean	WLS [30] mean
1	P&Q in (650-632)	0.0594	0.1982	0.1126	0.20
2	Current in (650-632)	0.0932	0.2241	0.1362	0.35
3	P&Q in (650-632) V at (671)	0.0322	0.1508	0.0900	not reported
4	P&Q in (650-632) P&Q in (633-634) P&Q in (671-692)	0.0301	0.0596	0.0450	not reported
5	P&Q in (650-632) P&Q in (633-634) P&Q in (671-692) V at (645)	0.0177	0.0492	0.0335	not reported

The quasi-real-time measurements of active/reactive power flows are presented in Table 1.

DSSE in the IEEE 13-bus system were considered, regarding (i) which of variables are monitored in real-time, i.e., number and place of real-time measurement devices, and (ii) the percent of errors for the pseudo-measurements and the errors for the real-time measurements.

The simulation results are shown in Table 2. Five different cases were considered. Each case was tested ten times. The mean absolute percentage error of bus voltage magnitude (MAPEV) is used to evaluate the performance of the different cases. The comparison of minimum, maximum, and mean value of MAPEV obtained over 10 runs is presented in Table 2 is evident that as the number of real-time monitored variables increases, the accuracy of the DSSE results is improved. Of course, this is quite logical. However, these results can help to determine which of the variable should be measure (power, current, voltage) as well as locations of real-time measurements to improve the DSSE performance.

The power measurement in the source branch (650-632) has a crucial impact on the accuracy of the results. Significant improvements of the DSSE performance are performed with additional real-time measurements of voltage magnitude at critical buses of the network and active and reactive power in the lateral branches. The results for Cases 1 and 2 presented in Table 2 are compared with those reported in [30]. As can be seen, the proposed PSOS-CGSA algorithm enables better DSSE results than the branch current-based WLS algorithm.

TABLE 3. Estimated and true values of the active power of load for the IEEE 13 bus system.

Bus	Phase A Estim.	Phase A True	Phase B Estim.	Phase B True	Phase C Estim.	Phase C True
634	159.99	160	119.99	120	119.99	120
645	-	-	172.57	170	-	-
646	-	-	233.75	230	-	-
671	386.09	385	386.09	385	386.09	385
611	-	-	-	-	178.79	170
652	128.01	128	-	-	-	-
692	-	-	-	-	170.4	170
675	484.95	485	67.99	68	289.97	290

TABLE 4. Estimated and true values of voltage magnitudes for the IEEE 13-bus test system.

Bus	Phase A Estim.	Phase A True	Phase B Estim.	Phase B True	Phase C Estim.	Phase C True
650	1.0000	1.0000	1.0000	1.0000	1.0000	1.0000
632	0.9498	0.9499	0.9840	0.9839	0.9300	0.9300
633	0.9466	0.9466	0.9820	0.9819	0.9271	0.9271
634	0.9207	0.9207	0.9625	0.9624	0.9064	0.9064
645	0	0	0.9745	0.9745	0.9284	0.9283
646	0	0	0.9728	0.9729	0.9264	0.9264
671	0.9110	0.9110	0.9876	0.9874	0.8716	0.8718
680	0.9111	0.9110	0.9876	0.9874	0.8717	0.8718
684	0.9094	0.9093	0	0	0.8682	0.8685
611	0	0	0	0	0.8648	0.8653
652	0.9044	0.9043	0	0	0	0
692	0.9111	0.9110	0.9876	0.9874	0.8717	0.8718
675	0.9027	0.9026	0.9888	0.9886	0.8678	0.8679

TABLE 5. Estimated and true values of voltage angles for the IEEE 13-bus test system.

Bus	Phase A Estim.	Phase A True	Phase B Estim.	Phase B True	Phase C Estim.	Phase C True
650	0.000	0.000	-120.000	-120.000	120.000	120.000
632	-2.746	-2.746	-121.683	-121.682	117.807	117.800
633	-2.822	-2.823	-121.733	-121.731	117.801	117.794
634	-3.607	-3.608	-122.246	-122.244	117.224	117.217
645	-	-	-121.869	-121.864	117.829	117.822
646	-	-	-121.944	-121.938	117.877	117.869
671	-5.904	-5.898	-122.200	-122.210	115.946	115.951
680	-5.904	-5.898	-122.199	-122.210	115.945	115.950
684	-5.957	-5.950	-	-	115.907	115.916
611	-	-	-	-	115.825	115.838
652	-5.880	-5.873	-	-	-	-
692	-5.904	-5.898	-122.199	-122.210	115.945	115.950
675	-6.083	-6.076	-122.294	-122.305	116.063	116.068

The detailed DSSE results for Case 5 are presented in Tables 3–5. The estimated and true values of active power for the IEEE 13-bus system are presented in Table 3. A maximum percentage error of 5.17 % corresponds to the estimated load at the bus 611, which is modeled by a constant current model. This error is calculated as: $error = \left|\frac{P^{true} - P^{est}}{P^{true}}\right| \cdot 100$. Tables 4 and 5 show the estimated and true values of the voltage magnitudes and the voltage angles for all three phases. As can be seen, the estimated voltage magnitudes and voltage angles match very well with the true values.

B. IEEE 37-BUS TEST SYSTEM

Detail network parameters for the IEEE 37-bus test system, presented in Figure 3, can be found in [28]. The proposed DSSE approach was tested on the IEEE 37-bus system with

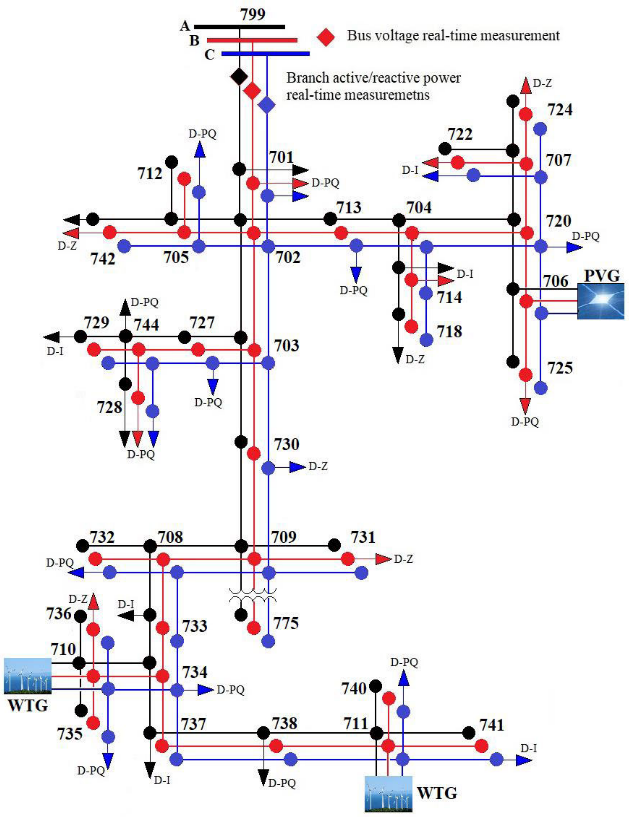

FIGURE 3. Three-phase diagram of the IEEE 37-bus test system.

TABLE 6. DG unit specifications.

Location	Type	P_{DG} (kW)			Power factor
		Phase A	Phase B	Phase C	
706	PVG	150	150	150	1
710	WTG	180	180	180	0.95
711	WTG	200	200	200	0.95

three renewable-based DG units whose specifications are given in Table 6. It is assumed that all DG units operate in PQ mode. The PVG operates at a unity power factor, whereas WTG operates at 0.95 lag power factors (absorbs reactive power) in all operating conditions.

The active and reactive powers of load given in [28] are considered as the forecasted mean values, which are used to generate pseudo-measurements according to (8). The active powers of the DG units given in Table 6 are assumed to represent their forecasted values calculated using the approach described in [22]. These forecasted outputs are used in (11) to obtain the pseudo-measurements of the output power of DG units.

The DSSE simulation was carried out on the IEEE 37-bus test system, assuming that there are available the real-time measurements of active/reactive power flows and bus voltages, as given in Table 7.

The DSSE results obtained by the proposed hybrid PSOS-CGSA algorithm were compared with two original well-established metaheuristic optimization algorithms, i.e., particle swarm optimization (PSO) [32] and gravitational

TABLE 7. Real-time measurements in the IEEE 37-bus system.

Location	Measurements	Phase A	Phase B	Phase C
Branch 799-701	P (kW)	336.930	151.237	406.076
	Q (kVAr)	676.835	493.386	420.749
Branch 702-713	P (kW)	-15.207	46.094	59.972
	Q (kVAr)	94.474	43.909	121.571
Branch 709-708	P (kW)	-45.312	-224.505	-171.811
	Q (kVAr)	265.648	313.364	137.909
Bus 709	V (pu)	0.9775	0.9877	0.9828

TABLE 8. Algorithms parameter settings.

PSO	C_1=2; C_2=2; w_{max}=0.9; w_{min}=0.4
GSA	G_0=1; α=20; p=2; K_0=1
PSOS	C_{1i}=0.5; C_{1f}=2.5; λ=0.0001; w_{max}=0.9; w_{min}=0.4
PPSO	-
CGSA	G_0=1; α=20; $wmax$=0.1; $wmin$=1e-10; Sinusoidal map
PSOGSA	C_1=2; C_2=2; G_0=1; α=20
PPSOGSA	G_0=1; α=20;
Proposed PSOS-CGSA	C_{1i}=0.5; C_{1f}=2.5; λ=0.0001; G_0=1; α=20; Sinusoidal map

TABLE 9. Statistical results of MAPEV (%) for the IEEE 37-bus system.

Algorithm	Min	Max	Mean	Std	TOC
PSO [32]	0.0262	0.1766	0.0815	0.0479	1.635
GSA [27]	0.0483	0.1738	0.1059	0.0459	1.469
PSOS [24]	0.0107	0.0833	0.0436	0.0244	1.477
CGSA [25]	0.0168	0.1445	0.0771	0.0407	1.549
PPSO [31]	0.0164	0.1279	0.0447	0.0336	1.548
PSOGSA [23]	0.0199	0.1448	0.0533	0.0395	1.523
PPSOGSA [22]	0.0165	0.0819	0.0445	0.0200	1.602
Proposed PSOSCGSA	0.0068	0.0303	0.0181	0.0092	1.508

search algorithm (GSA) [27]; several recently proposed innovated versions of these techniques such as particle swarm optimization with sigmoid-based acceleration coefficients (PSOS) [24], chaos-based gravitational search algorithm (CGSA) [25], phasor particle swarm optimization (PPSO) [31]; and their hybrids such as hybrid particle swarm optimization and gravitational search algorithm (PSOGSA) [23], and hybrid phasor particle swarm optimization and gravitational search algorithm (PPSOGSA) [22].

The parameters used in the simulation are presented in Table 8. These parameters were adopted based on their default values in noted references. The population size and maximum iteration number are set as; $(N) = 25$ and $(t_{\max}) = 100$ for all case studies, including the IEEE 13-bus test system.

The statistical indicators of MAPEV for DSSE in the IEEE 37-bus system using different optimization methods are presented in Table 9. The results shown in Table 9 correspond to the MAPEV values obtained over 10 consecutive DSSE runs using each of the algorithms, as shown in Figure 4. The sixth column of Table 9 presents the time of computation (TOC) per iteration. These results show that there is no significant difference in the calculation time between the different algorithms. This is quite expected, given that these are algorithms of similar structure, which is explained in Section 4.

The results presented in Table 9 and Figure 4 clearly indicate that the proposed hybrid PSOS-CGSA algorithm

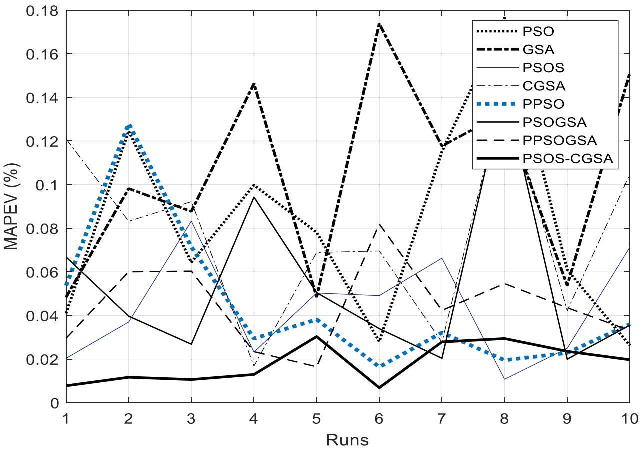

FIGURE 4. The variation range of MAPEV.

TABLE 10. Voltage magnitudes in the IEEE 37-bus system.

Bus	Phase A		Phase B		Phase C	
	Estim.	True	Estim.	True	Estim.	True
799	1.0000	1.0000	1.0000	1.0000	1.0000	1.0000
701	0.9893	0.9893	0.9935	0.9935	0.9900	0.9901
702	0.9846	0.9845	0.9904	0.9904	0.9857	0.9857
703	0.9799	0.9798	0.9876	0.9875	0.9832	0.9832
730	0.9780	0.9779	0.9877	0.9876	0.9828	0.9827
709	0.9776	0.9775	0.9877	0.9877	0.9828	0.9828
775	0.9775	0.9773	0.9877	0.9876	0.9831	0.9830
708	0.9771	0.9769	0.9881	0.9881	0.9833	0.9833
732	0.9768	0.9766	0.9881	0.9881	0.9830	0.9829
733	0.9767	0.9765	0.9885	0.9885	0.9840	0.9839
734	0.9765	0.9764	0.9898	0.9898	0.9851	0.9851
737	0.9755	0.9754	0.9898	0.9898	0.9861	0.9860
738	0.9756	0.9756	0.9905	0.9906	0.9866	0.9866
711	0.9763	0.9763	0.9919	0.9920	0.9872	0.9872
741	0.9761	0.9761	0.9920	0.9921	0.9871	0.9871
740	0.9760	0.9760	0.9920	0.9921	0.9869	0.9869
710	0.9791	0.9789	0.9927	0.9927	0.9867	0.9867
735	0.9787	0.9786	0.9927	0.9927	0.9864	0.9863
736	0.9791	0.9789	0.9914	0.9914	0.9856	0.9856
731	0.9776	0.9775	0.9871	0.9870	0.9821	0.9821
727	0.9788	0.9786	0.9868	0.9867	0.9825	0.9825
744	0.9782	0.9780	0.9862	0.9861	0.9823	0.9822
728	0.9778	0.9776	0.9858	0.9857	0.9819	0.9818
729	0.9779	0.9777	0.9860	0.9858	0.9823	0.9822
713	0.9843	0.9842	0.9899	0.9899	0.9847	0.9847
704	0.9844	0.9844	0.9892	0.9892	0.9839	0.9838
720	0.9857	0.9857	0.9894	0.9893	0.9827	0.9827
706	0.9876	0.9876	0.9909	0.9908	0.9841	0.9841
725	0.9877	0.9876	0.9906	0.9905	0.9838	0.9838
707	0.9852	0.9851	0.9852	0.9851	0.9788	0.9787
722	0.9851	0.9851	0.9848	0.9847	0.9784	0.9783
724	0.9851	0.9851	0.9845	0.9843	0.9781	0.9780
714	0.9842	0.9842	0.9890	0.9889	0.9838	0.9838
718	0.9832	0.9831	0.9881	0.9880	0.9839	0.9838
705	0.9837	0.9837	0.9896	0.9895	0.9842	0.9841
712	0.9833	0.9832	0.9896	0.9895	0.9837	0.9836
742	0.9837	0.9836	0.9889	0.9888	0.9837	0.9836

provides more accurate and stable DSSE compared to other metaheuristic algorithms over a wide range of test runs, which proves its robustness.

The estimated and true values of active power for the IEEE 37-bus system obtained by the proposed PSOS-CGSA algorithm are presented in Figures 5-7. A maximum percentage error of 8.25 % corresponds to the estimated load in phase A at the bus 733. Table 10 shows the estimated and true values of voltage magnitudes. As can be seen from this table, the estimated voltages match very well with the true values.

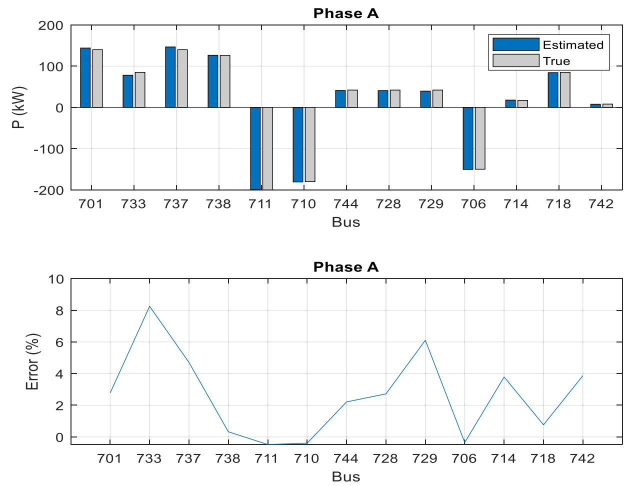

FIGURE 5. Active power in phase A for the IEEE 37-bus system.

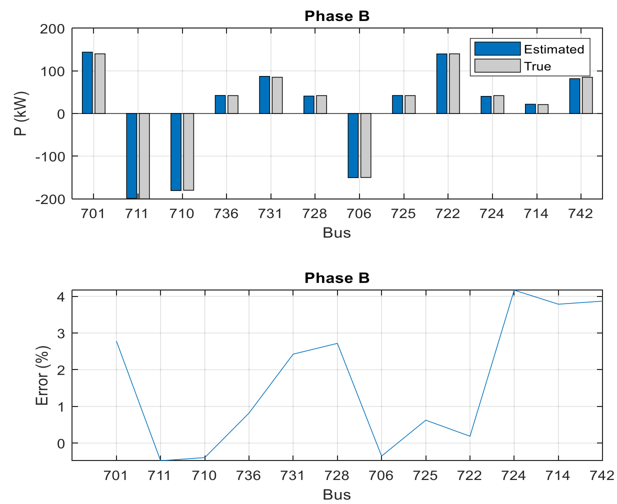

FIGURE 6. Active power in phase B for the IEEE 37-bus system.

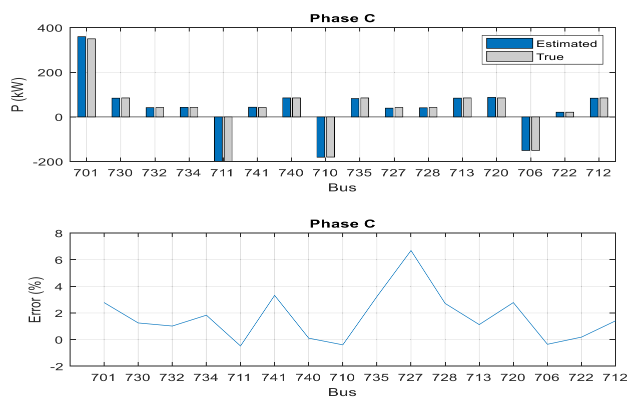

FIGURE 7. Active power in phase C for the IEEE 37-bus system.

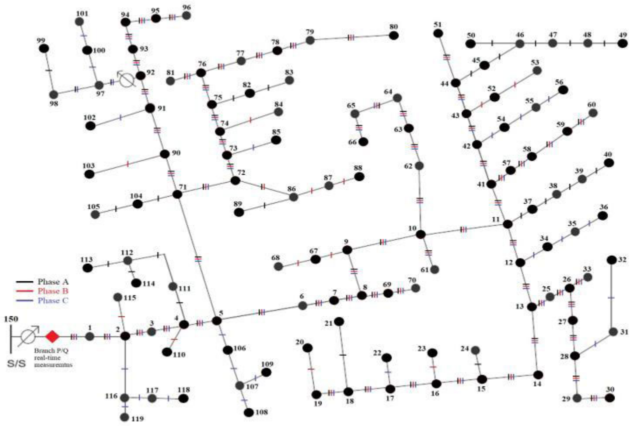

FIGURE 8. Active One-line diagram of the IEEE 123-bus system.

TABLE 11. Simulation results of DSSE for the IEEE 123-bus system.

Real-time measurements	MAPEV (%)		MAPEA (%)	
	Proposed PSOS-CGSA	WLS [30]	Proposed PSOS-CGSA	WLS [30]
P&Q in (150-1)	0.079	0.15	0.047	0.09
P&Q in (5-71)	0.082	0.16	0.059	0.09
P&Q in (43-44)	0.099	0.17	0.071	0.09

C. IEEE 123-BUS TEST SYSTEM

In order to evaluate the efficiency of the proposed DSSE methodology in larger systems, the IEEE 123-bus test feeder is considered. The single diagram is shown in Figure 8. The proposed PSOS-CGSA method was successfully implemented on the IEEE-123 system using system data are taken from [28].

The simulation results for the IEEE 123-bus system are presented in Table 11. The mean absolute percentage error of bus voltage magnitude (MAPEV) and bus voltage angle (MAPEA) are used to evaluate the performance of the proposed method in comparison to the results reported in [30]. DSSE is considered regarding to which of variables are monitored in real-time. Note that, one real-time measurement in different locations with all pseudo-measurements is tested, as in [30]. It can be seen that the DSSE results obtained from the PSOS-CGSA algorithm are better than those obtained from the branch current-based WLS algorithm [30]. This clearly indicates that the proposed approach can be effectively used for DSSE in large-scale distribution systems.

VI. CONCLUSIONS

In this paper, a novel PSOS-CGSA method based metaheuristic optimization for three-phase DG-integrated DSSE has been proposed and verified on the IEEE 13-bus, 37-bus, and 123-bus test systems. The simulation results imply conclusions which can be summarized a follows:

- The proposed model provides a reliable and sufficient accurate state estimation results in DG-integrated distribution networks with a very limited number of real-time measurements at the source substation.
- Significant improvements of the DSSE results can be achieved with additional real-time measurements in the lateral branches.
- The proposed hybrid PSOS-CGSA algorithm provides more accurate and stable DSSE compared to other algorithms.
- The DSSE model can be easily implemented for any distribution system, without limitation in terms of dimension, topology, level of loads, and type of DG units.

REFERENCES

[1] S. Nanchian, A. Majumdar, and B. C. Pal, "Three-phase state estimation using hybrid particle swarm optimization," *IEEE Trans. Smart Grid*, vol. 8, no. 3, pp. 1035–1045, May 2017.

[2] A. Primadianto and C.-N. Lu, "A review on distribution system state estimation," *IEEE Trans. Power Syst.*, vol. 32, no. 5, pp. 3875–3883, Sep. 2017.

[3] G. Wang, G. B. Giannakis, J. Chen, and J. Sun, "Distribution system state estimation: An overview of recent developments," *Frontiers Inf. Technol. Electron. Eng.*, vol. 20, no. 1, pp. 4–17, Jan. 2019.

[4] R. Singh, R. A. Jabr, and B. C. Pal, "Choice of estimator for distribution system state estimation," *IET Gener., Transmiss. Distrib.*, vol. 3, no. 7, pp. 666–678, Jul. 2009.

[5] A. Ranković, B. M. Maksimović, and A. T. Sarić, "A three-phase state estimation in active distribution networks," *Int. J. Electr. Power Energy Syst.*, vol. 54, pp. 154–162, Jan. 2014.

[6] P. M. De Oliveira-De Jesus and C. Henggeler Antunes, "A detailed network model for distribution systems with high penetration of renewable generation sources," *Electr. Power Syst. Res.*, vol. 161, pp. 152–166, Aug. 2018.

[7] M. Majidi, M. Etezadi-Amoli, H. Livani, and M. S. Fadali, "Distribution systems state estimation using sparsified voltage profile," *Electr. Power Syst. Res.*, vol. 136, pp. 69–78, Jul. 2016.

[8] M. Majidi, M. Etezedi-Amoli, and H. Livani, "Distribution system state estimation using comprehenssive sensing," *Elect. Power Energy Syst.*, vol. 88, pp. 175–186, Jun. 2017, doi: 10.1016/j.ijepes.2016.12.016.

[9] F. Ni, P. H. Nguyen, J. F. G. Cobben, H. E. Van den Brom, and D. Zhao, "Three-phase state estimation in the medium-voltage network with aggregated smart meter data," *Int. J. Electr. Power Energy Syst.*, vol. 98, pp. 463–473, Jun. 2018.

[10] M. M. Othman, M. H. Ahmed, and M. M. A. Salama, "A novel smart meter technique for voltage and current estimation in active distribution networks," *Int. J. Electr. Power Energy Syst.*, vol. 104, pp. 301–310, Jan. 2019.

[11] M. F. Medeiros Júnior, M. A. D. Almeida, M. C. S. Cruz, R. V. F. Monteiro, and A. B. Oliveira, "A three-phase algorithm for state estimation in power distribution feeders based on the powers summation load flow method," *Electr. Power Syst. Res.*, vol. 123, pp. 76–84, Jun. 2015.

[12] T. Soares, U. Bezerra, and M. Tostes, "Full-observable three-phase state estimation algorithm applied to electric distribution grids," *Energies*, vol. 12, no. 7, p. 1327, Apr. 2019.

[13] F. Ahmad, M. Tariq, and A. Farooq, "A novel ANN-based distribution network state estimator," *Int. J. Electr. Power Energy Syst.*, vol. 107, pp. 200–212, May 2019.

[14] J.-H. Menke, N. Bornhorst, and M. Braun, "Distribution system monitoring for smart power grids with distributed generation using artificial neural networks," *Int. J. Electr. Power Energy Syst.*, vol. 113, pp. 472–480, Dec. 2019.

[15] G. Cheng, S. Song, Y. Lin, Q. Huang, X. Lin, and F. Wang, "Enhanced state estimation and bad data identification in active power distribution networks using photovoltaic power forecasting," *Electr. Power Syst. Res.*, vol. 177, Dec. 2019, Art. no. 105974.

[16] K. Liu, W. Sheng, and K. He, "Unbalanced three-phase distribution state estimation using cooperative particle swarm optimization," in *Proc. IEEE PES T&D Conf. Expo.*, Apr. 2014, pp. 14–17, Chicago, IL, USA.

[17] R. Khorshidi, F. Shabaninia, and T. Niknam, "A new smart approach for state estimation of distribution grids considering renewable energy sources," *Energy*, vol. 94, pp. 29–37, Jan. 2016.

[18] S. Khushalani, J. M. Solanki, and N. N. Schulz, "Development of three-phase unbalanced power flow using PV and PQ models for distributed generation and study of the impact of DG models," *IEEE Trans. Power Syst.*, vol. 22, no. 3, pp. 1019–1025, Aug. 2007.

[19] W. H. Kersting, *Distribution System Modeling and Analysis*. Boca Raton, FL, USA: CRC Press, 2002.

[20] S. Naka, T. Genji, T. Yura, and Y. Fukuyama, "A hybrid particle swarm optimization for distribution state estimation," *IEEE Power Eng. Rev.*, vol. 22, no. 11, p. 57, Nov. 2002.
[21] N. Katic, L. Fei, G. Svenda, and Z. Yongji, "Gield testing of distribution state estimator," in *Proc. 22nd Int. Conf. Electr. Distrib.*, Jun. 2013, pp. 1–4.
[22] Z. Ullah, S. Wang, J. Radosavljevic, and J. Lai, "A solution to the optimal power flow problem considering WT and PV generation," *IEEE Access*, vol. 7, pp. 46763–46772, 2019.
[23] S. Mirjalili and S. Z. M. Hashim, "A new hybrid PSOGSA algorithm for function optimization," in *Proc. Int. Conf. Comput. Inf. Appl.*, Dec. 2010, pp. 77–374.
[24] D. Tian, X. Zhao, and Z. Shi, "Chaotic particle swarm optimization with sigmoid-based acceleration coefficients for numerical function optimization," *Swarm Evol. Comput.*, vol. 51, Dec. 2019, Art. no. 100573.
[25] S. Mirjalili and A. H. Gandomi, "Chaotic gravitational constants for the gravitational search algorithm," *Appl. Soft Comput.*, vol. 53, pp. 407–419, Apr. 2017.
[26] J. Radosavljević, *Metaheuristic Optimization in Power Engineering*, 1st ed. London, U.K.: IET, 2018.
[27] E. Rashedi, H. Nezamabadi-Pour, and S. Saryazdi, "GSA: A gravitational search algorithm," *Inf. Sci.*, vol. 179, no. 13, pp. 2232–2248, Jun. 2009.
[28] *IEEE PES AMPS DSAS Test Feeder Working Group*. Accessed: Nov. 14, 2019. [Online]. Available: https://site.ieee.org/pes-testfeeders/resources/
[29] D. H. Tungadio, B. P. Numbi, M. W. Siti, and A. A. Jimoh, "Particle swarm optimization for power system state estimation," *Neurocomputing*, vol. 148, pp. 175–180, Jan. 2015.
[30] H. Wang and N. N. Schulz, "A revised branch current-based distribution system state estimation algorithm and meter placement impact," *IEEE Trans. Power Syst.*, vol. 19, no. 1, pp. 207–213, Feb. 2004.
[31] M. Ghasemi, E. Akbari, A. Rahimnejad, S. E. Razavi, S. Ghavidel, and L. Li, "Phasor particle swarm optimization: A simple and efficient variant of PSO," *Soft Comput.*, vol. 23, no. 19, pp. 9701–9718, Oct. 2019.
[32] J. Kennedy and R. C. Eberhart, "Particle swarm optimizaton," in *Proc. IEEE Int. Conf. Neural Netw.*, Perth, WA, Australia, Dec. 1995, pp. 48–1942.

ZIA ULLAH (Graduate Student Member, IEEE) received the bachelor's degree in electrical power from the University of Engineering and Technology, Lahore, Pakistan, in 2007, and the M.S. degree in electrical engineering from COMSATS University at Wah Campus, Pakistan, in 2015. He is currently pursuing the Ph.D. degree with the Department of Electrical and Electronics Engineering, Huazhong University of Science and Technology (HUST), Wuhan, China. His research interests include power system optimization and the planning optimization of renewable energy resources and distributed generation.

MOHAMED R. ELKADEEM (Graduate Student Member, IEEE) received the B.S. and M.S. degrees in electrical engineering from the Faculty of Engineering, Tanta University, Tanta, Egypt, in 2012 and 2016, respectively. He is currently pursuing the Ph.D. degree with the Department of Electrical and Electronics Engineering, Huazhong University of Science and Technology, Wuhan, China. From 2013 to 2018, he was a Research Assistant Lecturer with the Faculty of Engineering, Tanta University. His research interests include hybrid renewable energy systems planning and design, power system optimization, distribution automation systems, and reliability analysis.

SHAORONG WANG was born in 1960. He received the B.E. degree in electrical engineering from Zhejiang University, Hangzhou, China, in 1984, the M.E. degree in electrical engineering from North China Electric Power University (NCEPU), Baoding, China, in 1990, and the Ph.D. degree in electrical engineering from the Huazhong University of Science and Technology (HUST), Wuhan, China, in 2004. He is currently a Professor with the HUST. His current research interests include smart grids, power system operation and control, wind power, renewable energy, and distributed generation.

JORDAN RADOSAVLJEVIĆ received the B.Sc. degree from the Faculty of Electrical Engineering, University of Priština at Kosovska Mitrovica, Kosovska Mitrovica, Serbia, in 1998, the M.Sc. degree from the Faculty of Electrical Engineering, University of Belgrade, in 2003, and the Ph.D. degree from the Faculty of Technical Sciences, University of Priština, in 2009. He is a Full Professor with the Department of Electrical and Computer Engineering, Faculty of Technical Sciences, University of Priština. His main research interests include power system analysis and control, power system optimization, renewable energy, and distributed generation.